The Stress Corrosion Cracking Behaviour Of Copper In Acetate Solutions

NWMO TR-2008-21 December 2008

C.D. Litke[1] and B.M. Ikeda[2]

[1] Atomic Energy of Canada Limited
[2] University of Ontario Institute of Technology

nwmo
NUCLEAR WASTE MANAGEMENT ORGANIZATION
SOCIÉTÉ DE GESTION DES DÉCHETS NUCLÉAIRES

Nuclear Waste Management Organization
22 St. Clair Avenue East, 6th Floor
Toronto, Ontario
M4T 2S3
Canada

Tel: 416-934-9814
Web: www.nwmo.ca

The Stress Corrosion Cracking Behaviour of Copper in Acetate Solutions

NWMO TR-2008-21

December 2008

C.D. Litke[1] and B.M. Ikeda[2]

[1] Atomic Energy of Canada Limited
[2] University of Ontario Institute of Technology

ABSTRACT

Title: **The Stress Corrosion Cracking Behaviour of Copper in Acetate Solutions**
Report No.: **NWMO TR-2008-21**
Author(s): C.D. Litke[1] and B.M. Ikeda[2]
Company: [1] Atomic Energy of Canada Limited
[2] University of Ontario Institute of Technology
Date: December 2008

Abstract
This study investigated the effect of solution concentration, aeration, applied current and extension rate on the stress corrosion cracking (SCC) behaviour of oxygen-free phosphorous-doped copper in pH 9 acetate solutions. The constant extension rate tests were performed at room temperature using a compact tension specimen under a galvanically applied current. The corrosion potential was measured during all experiments. The findings are summarized as follows:

- In a range of acetate concentrations between 0.15 mol·L^{-1} and 0.5 mol·L^{-1}, SCC was not observed on specimens exposed to an applied current of 1 µA·cm^{-2}.
- In the 0.2 mol·L^{-1} acetate concentration, neither the presence of air in the solution nor an increase in current density to 2 µA·cm^{-2} introduced SCC.
- In the 0.5 mol·L^{-1} acetate concentration, a decrease in extension rate did not produce SCC.

The stress corrosion cracking factor, surface crack extension rate, and visual examination of the copper specimens suggested predominantly ductile behaviour under the range of acetate concentrations, solution conditions, applied current densities, and extension rates studied.

TABLE OF CONTENTS

LIST OF FIGURES

Page

LIST OF TABLES

Page

1. INTRODUCTION

Oxygen-free phosphorous-doped (OFP) copper has been selected as the corrosion-barrier material for the used-fuel containers that would be used to contain and isolate used fuel in a deep geological repository (DGR) (Maak 1999).

Stress corrosion cracking (SCC) is a well-known phenomenon for copper and copper alloys. Three conjoint factors are required for SCC: a susceptible material, an appropriate environment, and sufficient tensile stress. In previous Canadian studies, experiments were carried out to investigate the SCC behaviour in acetate environments (Litke and Ikeda 2006). In a DGR, SCC agents such as acetate could be formed by gamma-radiolysis or microbial activity (King and Litke 1997). Copper has been shown to be susceptible to SCC in acetate environments (Cassange et al. 1990, Honda et al. 1999).

Previous studies indicated that a Cu_2O/CuO surface oxide film must be present for SCC to occur. The formation of the surface oxide film depends on the potential of the system. A stress corrosion cracking model has been developed for predicting the occurrence of SCC on copper containers in a DGR (King and Kolar 2005). The model accounts for SCC of copper containers due to the presence of SCC agents and a corrosion potential that promotes the formation of the surface oxide film.

The purpose of this project is to develop experimental copper SCC data that can be employed together with the SCC model, to support the assumption that stress corrosion cracking will not have a significant impact on the integrity or long-term performance of a copper used-fuel container during its design lifetime in a DGR. The objectives of the SCC program within the NWMO Technical Research and Development Program are to:

i) Improve our knowledge and understanding of the conditions which may lead to SCC of copper in a deep geologic repository for used fuel; and

ii) Determine the boundaries for the environmental parameters affecting SCC of copper.

This report describes the results of room temperature constant-extension rate tests performed in solutions containing acetate, which is one of the SCC agents. These tests were designed to study the effect of acetate concentration, aeration, applied current, and extension rate on the SCC of OFP copper material previously obtained from the SKB.

2. EXPERIMENTAL

2.1 MATERIALS AND SPECIMENS

Compact tension (CT) coupons were prepared from section C1E of the SKB-4 OFP copper plate. The location of section C1 in plate SKB-4 was described previously (Ikeda and Litke 2000). The pre-crack was generated using a carefully regulated fatigue crack-growth procedure with an MTS Universal Testing machine. All specimens tested had the fatigue crack oriented in the (T-S) orientation (Figure 1).

The overall shape of the CT specimens follows the specification outlined in ASTM-E 399-90 (ASTM 1994). The ratio of the specimen dimensions conform to this standard, but because of the low strength of copper, the overall dimensions do not. The standard requires physically larger specimens to be used to maintain appropriate plane-strain fracture conditions for a low strength material such as copper. Such specimens would be unreasonable for laboratory testing. The overall SCC behaviour can be compared for a consistent set of specimens although the estimated (ASTM 1994) stress intensity factor (K_Q) and crack velocity are not strictly valid for the application of plane strain fracture mechanics. The values may be used to qualitatively compare the crack growth for various environmental and loading conditions. Ductile tearing and measurement errors caused by the loss of surface planarity will contribute to the estimated values for the surface crack velocity (SCER) and K_Q for the onset of SCC reported here.

2.2 EQUIPMENT

2.2.1 Constant Extension Rate Tests

The constant extension rate test (CERT) involves a continuous loading of the specimen by increasing the distance between the loading holes at constant rate. These experiments were performed in the slow strain rigs described previously (e.g., Ikeda and Litke 2000). A registered, small-volume pressure vessel with a PTFE liner was used as the cell body. The internal arrangement of the vessel was the same as reported previously for room temperature experiments (King et al. 1999a). CONAX pressure fittings with PTFE inner-sealing ferrules were used to permit electrode connections to penetrate the pressure vessel head yet maintain both electrical isolation and the pressure boundary seal.

All experiments reported were performed in ~0.5 L of solution at room temperature (22°C) and the specimens were pulled at a constant cross-head speed of 8.5×10^{-6} mm·s^{-1}, with the exception of CERT112 which was pulled at a rate of 3.4×10^{-6} mm·s^{-1}. A summary of the experimental conditions is presented in Table 1.

The experiments were performed under galvanostatic conditions using a platinum mesh counter electrode and a Thompson Ministat to apply the constant current, as described previously (e.g., King et al. 1999a). The potentials were measured against a commercially available saturated calomel electrode (SCE) and all potentials are reported against this electrode. The redox potential was not measured during the galvanostatic experiments. However, at the end of these experiments, but before opening the vessel to the atmosphere, the current was removed from the specimens and the counter electrode was allowed to re-equilibrate with the test solution. The potential of the platinum mesh was measured against the SCE and the value recorded as the final solution redox potential.

2.3 SOLUTIONS

The experiments were performed in deaerated or naturally aerated solutions containing sodium acetate. Four acetate concentrations (0.15, 0.2, 0.3 and 0.5 mol·L^{-1}) were used for the experiments performed in 2008. The acetate solutions were prepared by dissolving the appropriate mass of reagent grade sodium acetate salt in millipore purified deionised water, then adjusting the pH to 9.0 using dilute sodium hydroxide (NaOH) solution. The pH was

measured using a commercial glass pH electrode. The pH electrode was calibrated before each measurement using commercially available pH standards for pH 4, 7 and 10. The solution was poured into the cell body, and argon gas was bubbled through the solutions for at least 20 minutes before closing the cell. Purging with argon was not performed for experiment CERT118 (air test).

2.4 POST-TEST ANALYSES

Following the experiment, aliquots of the test solution were submitted for chemical analysis: by ion-coupled plasma spectroscopy to determine the total dissolved copper concentrations; and by ion chromatograph to ascertain the chloride concentration.

At the end of each experiment, a visual examination of the specimen was performed and features were noted. The specimen was then digitally imaged, and the images printed and stored for future reference. The images may not adequately represent the trueness of colour or the observed features reported in Table 2. The crack extension and crack-mouth opening values were measured from the overview sample image. The stress intensity factor (K_Q) at the onset of cracking was estimated using the initial surface fatigue crack length and the 5% secant load (ASTM 1994). The ratio of the specimen opening to the crack extension has been found to be an empirical indication of SCC and this stress corrosion cracking factor (SCCF1), along with the surface crack extension rate (SCER), was calculated as described previously (Ikeda and Litke 2000).

3. RESULTS AND DISCUSSION

A summary of the data for the experiments performed in 2008 is presented in Table 1. The data for all experiments in acetate solutions, including previous experiments, are shown in Table 2.

3.1 GENERAL OBSERVATIONS

The stress corrosion cracking factor (SCCF1) and the surface crack extension rates (SCER) are considered as indicators of crack growth behaviour.

Previous SCC experimental studies indicated that high values (> 5) of stress corrosion factor (SCCF1) would represent purely ductile behaviour, and very low SCCF1 values (< 2.5) would represent brittle-like SCC. Intermediate values of SCCF1 would indicate a mixture of brittle-like and ductile cracking behaviour. For intermediate values of SCCF1, detailed visual examination of the crack would be required to determine the degree of brittle-like behaviour (Litke and Ikeda 2006).

In previous SCC experimental studies low surface crack extension rates (SCER) of about 2 $nm \cdot s^{-1}$ also indicated purely ductile behaviour. High SCER values (> 2 $nm \cdot s^{-1}$) would indicate SCC.

In the present study, experiments were carried out in the range of 0.15 to 0.5 mol·L^{-1} acetate solutions. As shown in Table 1, the SCCF1 values of all experiments were found to be very close to or greater than 5, indicating purely ductile behaviour and no SCC. In addition, the SCER values of all experiments were found to be about 2, which also indicate purely ductile behaviour and no SCC (Table 1).

Visual examination of the copper SCC test specimens also revealed only ductile behaviour and no indications of SCC (Figures 2, 3, 7 and 8).

3.2 EFFECT OF ACETATE CONCENTRATION

This series of tests was carried out to study the effect of higher acetate concentrations on SCC of OFP copper using 1 μA·cm^{-2} galvanostatic current. The acetate concentrations were varied from 0.15 mol·L^{-1} to 0.5 mol·L^{-1}. The results are summarized in Table 1 and comparisons with previous work are provided in Table 2. The specimen surface and crack overview images are shown in Figures 2 and 3 respectively, while the load-and potential-transient plots are shown in Figure 4. The simple indicators (SCCF1 and SCER values) used to categorize SCC in ammonia and nitrite, were not adequate to fully categorize the type of SCC observed in the acetate experiments. An extensive visual characterization was performed.

The behaviour of OFP copper in 0.001, 0.01 and 0.1 mol·L^{-1} acetate (CERT97, CERT93, and CERT92 respectively) has been described previously (Ikeda and Litke 2006). The behaviour of OFP copper in acetate concentrations from 0.15 to 0.5 mol·L^{-1} (Table 1) was somewhat similar. The presence of small cracks in the region around the crack tip indicated the conditions were conducive to crack initiation, but were insufficient to maintain SCC crack propagation. Ductile tearing of the crack was more prominent than brittle-like SCC. The overall ductility of the specimen is indicated by the rounded region at the middle of the bottom edge of the specimen (Figure 2(ii)). The ductile tearing of the specimen is characterized by the generally rounded appearance of the region above the crack, as illustrated by the curved line drawn in Figure 2(ii).

At low acetate concentrations, a bright purple film was observed. The colour gradually disappeared and gave way to a light tarnish with a somewhat mottled blue/grey and red/brown appearance as the acetate concentration increased from 0.001 to 0.1 mol·L^{-1} (Figure 2). As the acetate concentration increased further, a dark, brown/black film appeared and covered the underlying surface layer. The thickness and uniformity of the film appeared to increase with increasing the time of the test rather than just with increasing the acetate concentration from 0.15 to 0.5 mol·L^{-1}. The film changed from sporadically covered (a mottled appearance) after 239 h (CERT117), to partially covered after 330 to 350 h (CERT115, CERT116), to fully covered after 503 h (CERT119). In 0.5 mol·L^{-1} acetate (CERT113) the film was quite thick and dark after 622 h and some of the film in the ductile zone flaked away. The gradual change in surface colour from purple, to pink, orange, and red, and finally to black, is consistent with a change in both the oxide composition and thickness. Pure, crystalline cuprous oxide (Cu_2O) is a deep, lustrous red whilst pure, crystalline cupric oxide (CuO) is black. The thin, adherent films may be either Cu_2O or CuO grown directly on the bare copper surface (a solid state growth mechanism). The oxidation state of the copper will depend upon the electrochemical potential for the oxidation reaction (e.g., Figure A.1: Pourbaix Diagram for Copper Ammonia Species at High pH in Ikeda and Litke 2004). As the film grows, the tarnish layer develops by precipitation of copper from solution (Bertocci et al. 1990). A thick film grown by precipitation

from solution may be less adherent. The black film can be associated with CuO, which as a thin film is adherent to the surface, but will flake off as it thickens.

Views of the specimens looking down the crack are shown in Figure 3. The crack tip is in the centre of the image. As one moves from the centre of the image to the left or right, one crosses the crack surface, then the fatigue crack surface, and finally the machined surface of the specimen. The dark or out of focus regions in the images are the portions of the specimen away from the crack. The ductility of some specimens can be seen by the narrowing of the centre of the specimen and the bulging at the end. The crack down overviews (Figure 3) generally show a purple oxidation of the fatigue crack with a purple/blue oxidation of the crack tip. The crack tips of the samples are blunted, but with occasional evidence for initiation cracks. In contrast, the crack-tip for CERT92 shows a predominantly porous red/brown oxidation (Figure 3 (iii)) and appears quite shredded. The overall sample surface view of CERT92 (Figure 2 (iii)), shows the presence of multiple small cracks, which suggests crack initiation without crack propagation.

CERT115 shows evidence of bright, freshly exposed surface at the crack tip (Figure 3 (vii)), which may corresponds to a -10 mV spike in the measured potential and a slight relaxation in the measured load at the end of the experiment (Figure 5). This feature appears to represent a view of the crack tip before the surface film has had time to re-grow.

A periodic sudden drop in load followed by a slow recovery has been observed previously for copper specimens exposed to nitrite and ammonia (Ikeda and Litke 2000, 2004). A sudden decrease in the applied load could be caused by the crack advancing or tearing thereby relieving the stress at the crack tip. This would open the crack and expose fresh copper surfaces along the crack front and the corrosion potential at the crack tip should shift to more negative potentials. A slow, positive-going potential shift could indicate an equilibration of the copper-water-oxide surface chemistry, i.e., film growth and dissolution. Although these observations are consistent with either a tarnish rupture (TR) type mechanism or a film rupture anodic dissolution (FRAD) mechanism for SCC, no SCC was observed in these experiments.

The possible effect of time on the appearance of the crack is illustrated by comparing experiments performed under the same conditions (CERT116 and CERT117 in Figures 3 (v) and (vi) respectively). Experiment CERT117 was 239 h long and showed the presence of multiple initiation cracks or “shredding” throughout the fracture surface, and little ductility (narrowing at the crack tip). In contrast, experiment CERT116 was 334 h long, and showed the presence of “shredding” along the edges of the crack surface, ductility and a blunt crack tip. This would suggest the crack initiation events occurred relatively early in the process, but did not propagate.

The shape of the load curves is consistent with the appearance of the region around the crack tip (Litke and Ikeda 2006). In general, the load curves were flat after the maximum load was attained (Figure 4). Experiment CERT92 showed some degree of brittle-like crack growth and the load curve correspondingly had the steepest decrease in slope. Unfortunately, experimental difficulties with the apparatus affected the recorded data for two of the experiments (CERT115 and CERT116). There was a loss in sample extension that allowed the specimen load to relax during the experiment (Figure 4 Aii). Upon restarting the pull, the load quickly returned to the value observed before the experiment was suspended. Although the exact effect of the load relaxation on SCC is not known, a comparison of these results to additional experiments performed under comparable conditions shows sufficient similarity to

suggest that the load relaxation did not affect the propagation of SCC. Experiment CERT117 was performed under the same experimental conditions as CERT116, with the sample for CERT117 having a longer initial crack length (2.95 mm) than that for CERT116 (2.59 mm). The overall shape of the load curves were similar, with CERT117 having a lower maximum load, as expected for a specimen with less initial load-bearing area.

The potential transient plots generally showed a negative shift in the steady state potential with increasing acetate concentration. However, the steady state potentials were similar for acetate concentrations between the 0.15 and 0.5 mol L^{-1}. This agrees with the observed film appearance at these acetate concentrations. An S-shaped curve appeared during the first 60 h of the 0.1 mol·L^{-1} and higher acetate concentration tests. The potential of the plateau after the S-shaped curve ranged from 80 mV in 0.15 mol·L^{-1} acetate to 50 mV in 0.5 mol·L^{-1} acetate, with the time at the plateau varying significantly.

The shape of the potential transient, and the value and duration of the plateau were thought to be significant precursors for SCC. A previous test (Litke and Ikeda 2006) in 0.1 mol·L^{-1} acetate with 0.001 mol·L^{-1} added chloride (CERT102, Figure 6) presented the strongest indications for SCC behaviour in acetate. The potential transient for CERT102 showed the same S-shaped curve, with a plateau value of ~ 80 mV for about 65 h duration. The load curve had the greatest decline after the maximum load, the crack extension was the longest observed for our acetate solutions, and the crack tip showed multiple crack initiations with some larger crack openings. However, the SCCF1 and SCER values were still in the mixed-mode cracking category with mainly ductile tearing and some brittle-like crack growth. Although the potential transient profiles for the 0.15 to 0.5 mol·L^{-1} acetate concentration series of experiments were similar in shape to CERT102, none of these experiments showed the prolonged time at the 80 mV plateau potential or evidence of SCC.

3.3 EFFECT OF AERATION

None of the deaerated experiments listed in Table 1 showed evidence of SCC, even though the potential transient profiles had the same shape as found for experiment CERT102 - described above. The absence of SCC suggests that the plateau after the S-shaped portion of the plot must attain a critical value and hold that value for a finite time. An increase in the plateau potential could be achieved by adjusting the oxidizing power of the environment. The presence of oxygen in the solution could induce more oxidizing conditions and drive SCC.

A test was carried out using aerated 0.2 mol·L^{-1} acetate under 1 $\mu A \cdot cm^{-2}$ galvanostatic current (CERT118). The solution was left open to the air for approximately 30 minutes (equivalent to the normal time for deaeration), before assembly. The results are compared to those from the corresponding deaerated case (CERT116). The specimen surface and crack images are shown in Figure 7A (i and ii) and 7B (i and ii) respectively, while the load- and potential-transient plots are shown in Figure 7C and 7D respectively.

The crack regions for the test specimens from experiments CERT116 and CERT118 both appeared generally rounded in the region above the crack indicating more ductile tearing of the crack than brittle-like SCC. The surface film on the CERT118 sample consisted of a heavier purple/brown oxide, while the CERT116 sample showed more of the darker brown/black oxide. In CERT118, the crack down view of the sample showed a heavier purple/blue oxidation and a visible shredding on the surfaces of the crack with blunting at the crack tip. In contrast, for

CERT116, the crack down view of the sample showed a red/brown to purple oxidation, a lesser degree of shredding and a much blunter crack tip.

The load curves from both experiments were similar (Figure 7C), but the potential-transient plots differed considerably (Figure 7D). Although both potential plots showed almost an identical initial S-shaped curve during the first 60 h, the potential values for CERT116 continued to climb to more positive values before gradually decaying back to values around 50 mV. The potentials in CERT118 remain more negative before recovering to the same 50 mV values. For the last 70 h of the tests, the potential values for both tests remain in the same range. The variation in the middle portion of the transients may correspond to the difference in the visible characteristics of the sample, but the effect was not sufficient to impact the final test outcomes.

Unfortunately, the CERT116 trace is tainted between 60 and 100 h because the motor stopped and the sample was not extended during that time. During this period, the load decreased and the sample relaxed. A positive increase in the measure sample potential also occurred during this period. The motor was restarted at ~ 100 h and both the load and potential values recovered. The CERT116 potential continued to decay to values around 50 mV.

3.4 EFFECT OF APPLIED CURRENT DENSITY

The steady state potential can be shifted to more positive values by increasing the applied current density, provided the corrosion process is either active or transpassive. A test was carried out in deaerated 0.2 $mol \cdot L^{-1}$ acetate, increasing the galvanostatic current to 2 $\mu A \cdot cm^{-2}$ (CERT120) from 1 $\mu A \cdot cm^{-2}$ (CERT116). The specimen surface and crack images are shown in Figure 7A (i and iii) and 7B (i and iii) respectively, while the load- and potential-transient plots are shown in Figure 7C and 7D.

The appearance of the two test specimens was similar, showing a generally rounded region above the crack indicating more ductile tearing of the crack than brittle-like SCC (Figures 7Ai and 7Aiii). The increase in experimental duration from 334 h (CERT116) to 456 h (CERT120) accounts for the difference in width for the region above the crack. In CERT120, more small cracks were seen in the region around the crack tip, indicating the conditions were more conducive to crack initiation than for CERT116, but were still insufficient to maintain SCC crack propagation.

The surface film in the CERT120 sample consisted of a heavier brown/black oxide that flaked away in the ductile zone, while the CERT116 sample had a similarly coloured film, but showed lighter and less uniform oxidation. The crack down views of both samples (Figures 7Bi and 7Biii) showed a red/brown to purple oxidation, but CERT120 had more red/brown oxidation and visible shredding. CERT116 showed more narrowing at the crack tip than CERT120, consistent with a much blunter crack tip.

The load curves from both experiments were similar in shape (Figure 7C). The maximum load for CERT120 was much lower than for CERT116, corresponding to the significantly longer fatigue crack in the CERT120 sample (3.02 mm vs. 2.59 mm for CERT116). The CERT120 potential-transient plot showed an initial S-shaped curve (Figure 7D) during the first 60 h. The potential value rose to a maximum of 80 mV and then decayed to a value around 65 mV, where it remained for the duration of the test. The potential did not plateau around the maximum value, as observed for other acetate experiments (Figures 4(B)). The absence, of a sustained

potential plateau near 80 mV and of SCC, is consistent with the observations that copper specimens tested in acetate displayed only ductile behaviour and no SCC. As described in the preceding section, the potential-transient for experiment CERT116 was tainted by a motor failure during the period where a potential plateau might have been observed.

The increase in current density to 2 $\mu A \cdot cm^{-2}$ and the corresponding positive values in the later stages of the potential-transient plot for CERT120 may account for the heavier oxide covering of the sample surface, the greater number of small cracks around the crack tip, and the enhanced shredding of the crack itself. However, the increase in current density was not sufficient to sustain the more positive potential values or to promote crack propagation.

3.5 EFFECT OF EXTENSION RATE

Previous work in acetate solutions showed the presence of small, secondary cracks on some of the largely ductile test specimens (Ikeda and Litke 2006). This observation suggested that initiation of SCC cracks could have occurred, but the extension rate was too fast to maintain SCC propagation. A decrease in the constant extension rate could allow more time for brittle-like SCC crack-tip conditions to be established, and for the crack to grow.

Experiments CERT112 and CERT113 were performed in 0.5 $mol \cdot L^{-1}$ acetate under 1 $\mu A \cdot cm^{-2}$ galvanostatic current. CERT112 used an extension rate of 3.4×10^{-6} $mm \cdot s^{-1}$, less than half of that used for CERT113 and in previous studies (8.5×10^{-6} $mm \cdot s^{-1}$). Neither specimen showed evidence of SCC, although indications of small cracks were seen in the areas below the fatigue crack in the crack overview images (Figure 2). In CERT112, the potential remained negative throughout the test and the final potential was only 2 mV. In CERT113, the potential remained positive throughout the test and the final potential was about 40 mV. These results suggested that the environment at the surface of a specimen during a faster extension rate test was different than at the lower extension rate, and that decreasing the extension rate did not increase the susceptibility to SCC.

4. CONCLUSION

Based on the SCC tests performed in this study and the assessment of previous SCC test results, findings can be summarized as follows:

- In a range of acetate concentrations between 0.15 $mol \cdot L^{-1}$ and 0.5 $mol \cdot L^{-1}$, SCC was not observed on specimens exposed to an applied current of 1 $\mu A \cdot cm^{-2}$.
- In the 0.2 $mol \cdot L^{-1}$ acetate concentration, neither the presence of air in the solution nor an increase in current density to 2 $\mu A \cdot cm^{-2}$ introduced SCC.
- In the 0.5 $mol \cdot L^{-1}$ acetate concentration, a decrease in extension rate did not produce SCC.

The stress corrosion factor (SCCF1), surface crack extension rate (SCER), and visual examination of the copper specimens suggested predominantly ductile behaviour under the

range of acetate concentrations, solution conditions, applied current densities, and extension rates studied. The results of these experiments clearly demonstrate the difficulty in inducing SCC on OFP copper in acetate solutions.

ACKNOWLEDGEMENTS

The authors wish to acknowledge the support and assistance of P. Maak of the Nuclear Waste Management Organization throughout this project. We also wish to acknowledge R. Herman for performing the chemical analysis, K.D. Jackson for instrumentation support, D.P. Godin for fatiguing the CT specimens, and J.P.L. David for the preparation of samples.

REFERENCES

ASTM. 1994. Standard test method for plane-strain fracture toughness of metallic materials, 1994 Annual Book of ASTM Standards, Section 3, Volume 03.01. American Society for Testing and Materials, Philadelphia, PA, E 399-90.

Bertocci, U., E.N. Pugh, and R.E. Ricker. 1990. "Environment-induced cracking of copper alloys". In Environment-Induced Cracking of Metals, NACE-10, (Editors R.P. Gangloff and M.B. Ives). National Association of Corrosion Engineers, Houston Tx. pp. 273-285.

Cassagne, T.B., J. Kruger, and E.N. Pugh. 1990. Role of the oxide film in the transgranular stress corrosion cracking of copper. In Environmentally Assisted Cracking: Science and Engineering, ASTM STP 1049. (Editors, W.B. Lisagor, T.W. Crooker, and B.N. Leis). American Society for Testing and Materials, Philadelphia, PA. pp. 59-75.

Honda, T., M. Yamashita, , M. Kamio, H. Uchida, and H. Shirai. 1999. Stress Corrosion Cracking of Pure Copper in Acetic Acid Solutions. IN 14th International Corrosion Congress, Cape Town, South Africa, September 26-October 1, 1999, pp. 19-67

Ikeda, B.M. and C.D. Litke. 2000. The effect of oxidant flux, nitrite concentration and chloride concentration on the stress corrosion cracking behaviour of non-welded and electron-beam welded copper. Prepared by Atomic Energy of Canada Limited for Ontario Power Generation. Ontario Power Generation, Nuclear Waste Management Division Report 06819-REP-01200-10049-R00. Toronto, Ontario.

Ikeda, B.M. and C.D. Litke. 2004. Status Report for 2003 on Stress Corrosion Cracking of OFP Copper in Ammonia. Prepared by Atomic Energy of Canada Limited for Ontario Power Generation. Ontario Power Generation, Nuclear Waste Management Division Report 06819-REP-01300-10078-R00. Toronto, Ontario.

King, F. and M. Kolar. 2005. Preliminary assessment of the stress corrosion cracking of used fuel disposal containers using the CCM-SCC.0 model. Ontario Power Generation, Nuclear Waste Management Division Report 06819-REP-01300-10103-R00. Toronto, Ontario.

King, F. and C.D. Litke. 1997. Stress corrosion cracking of copper – report on experimental methodologies and preliminary results. Prepared by Atomic Energy of Canada Limited for Ontario Hydro. Ontario Hydro, Nuclear Waste Management Division Report 06819-REP-01200-0010-R00. Toronto, Ontario.

King, F., C.D. Litke and B.M. Ikeda. 1999a. The effects of oxidant supply and chloride ions on the stress corrosion cracking of copper. Ontario Power Generation, Nuclear Waste Management Division Report 06819-REP-01200-10013-R00. Toronto, Ontario.

Litke, C.D., and B.M. Ikeda. 2006. The effect of acetate concentration, chloride concentration, and applied current on stress corrosion cracking of OFP copper. Ontario Power Generation, Nuclear Waste Management Division Report 06819-REP-01300-10005-R00. Toronto, Ontario.

Maak, P. 1999. The selection of a corrosion-barrier primary material for used-fuel disposal containers. Ontario Power Generation, Nuclear Waste Management Division Report 06819-REP-01200-10020 R00. Toronto, Ontario.

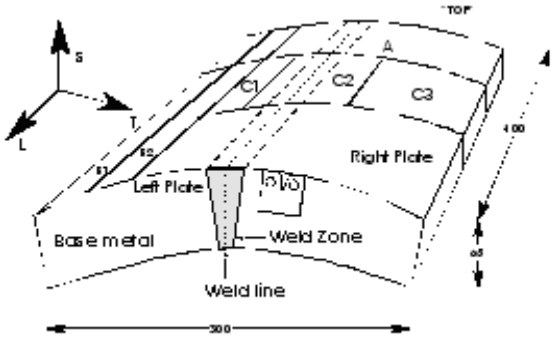

Figure 1: Schematic of SKB4 Plate Material Showing the Location of Specimen Cuts

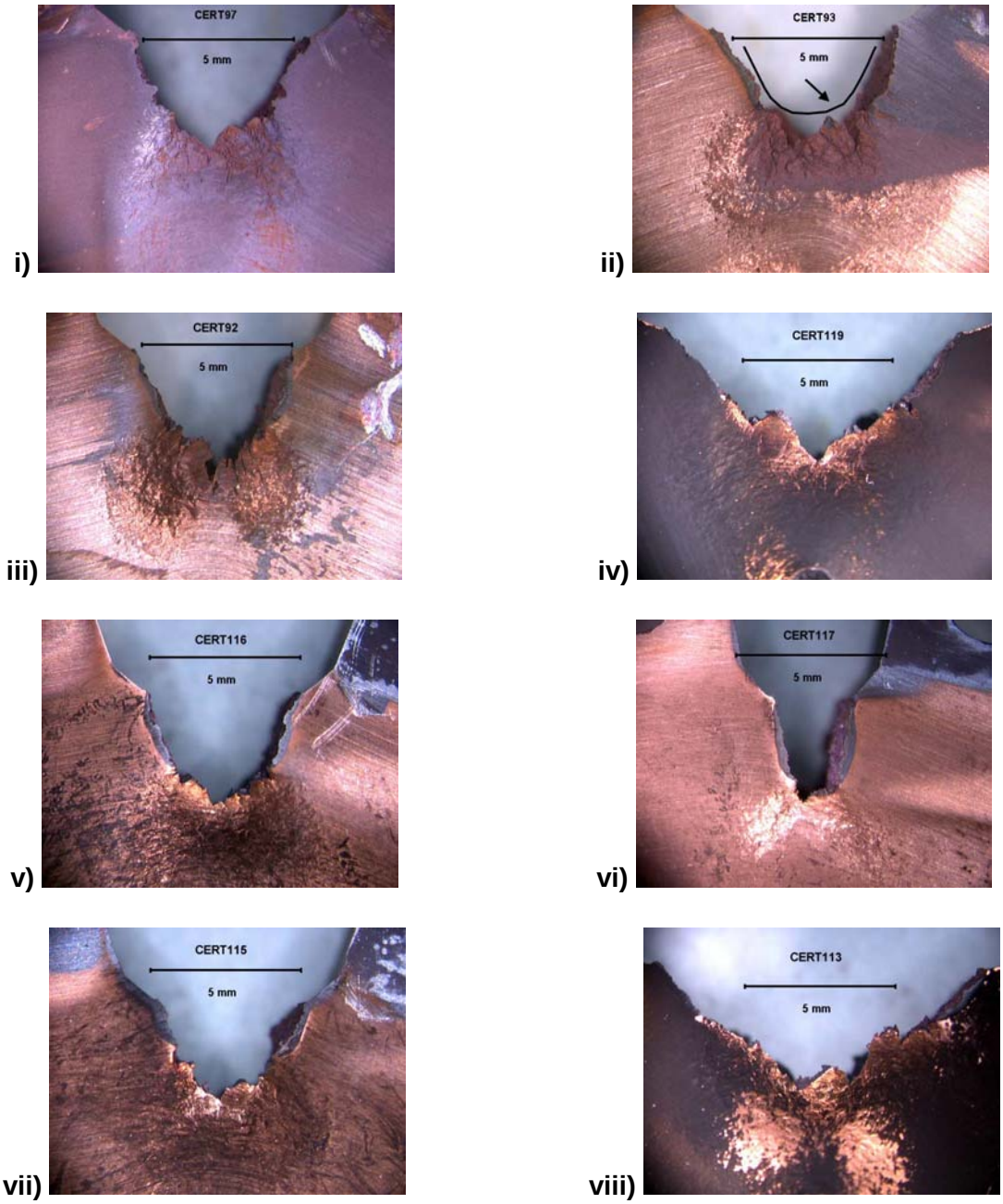

Figure 2: Macrographs of SKB4 Copper Plate Material CT Specimen Surfaces Showing The Effect of Acetate Concentration

Macrographs of CT specimen surface overviews (10X) following CERTs in various acetate concentrations: i) 0.001 mol·L^{-1} (CERT97), ii) 0.01 mol·L^{-1} (CERT93), iii) 0.1 mol·L^{-1} (CERT92), iv) 0.15 mol·L^{-1} (CERT119), v and vi) 0.2 mol·L^{-1} (CERT116 and CERT117), vii) 0.3 mol·L^{-1} (CERT115) and viii) 0.5 mol·L^{-1} (CERT113)

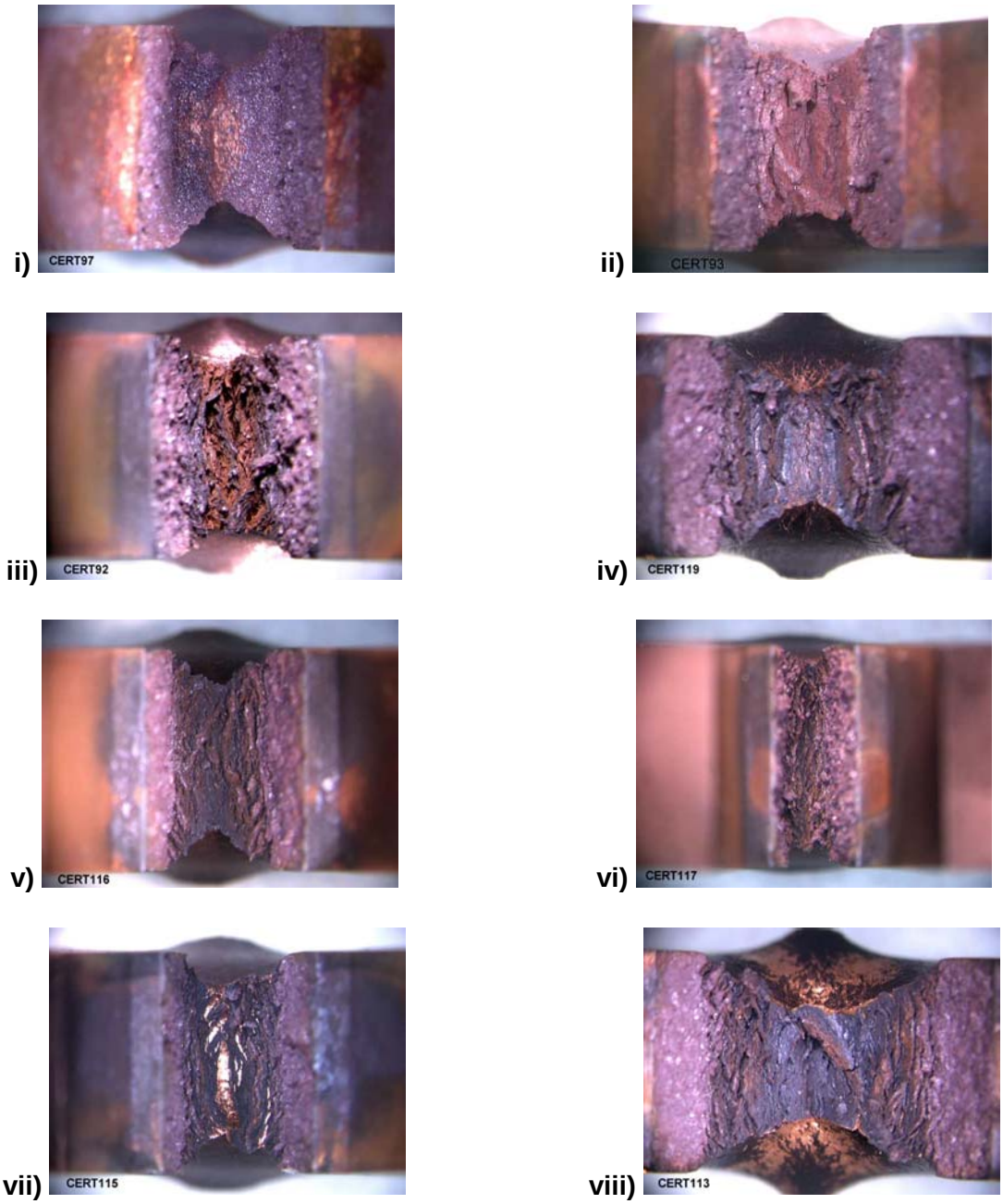

Figure 3: Macrographs of SKB4 Copper Plate Material CT Specimen Crack Overviews Showing The Effect of Acetate Concentration

Macrographs of CT specimen crack overviews (10X) following CERTs in various acetate concentrations: i) 0.001 mol·L^{-1} (CERT97), ii) 0.01 mol·L^{-1} (CERT93), iii) 0.1 mol·L^{-1} (CERT92), iv) 0.15 mol·L^{-1} (CERT119), v and vi) 0.2 mol·L^{-1} (CERT116 and CERT117), vii) 0.3 mol·L^{-1} (CERT115) and viii) 0.5 mol·L^{-1} (CERT113)

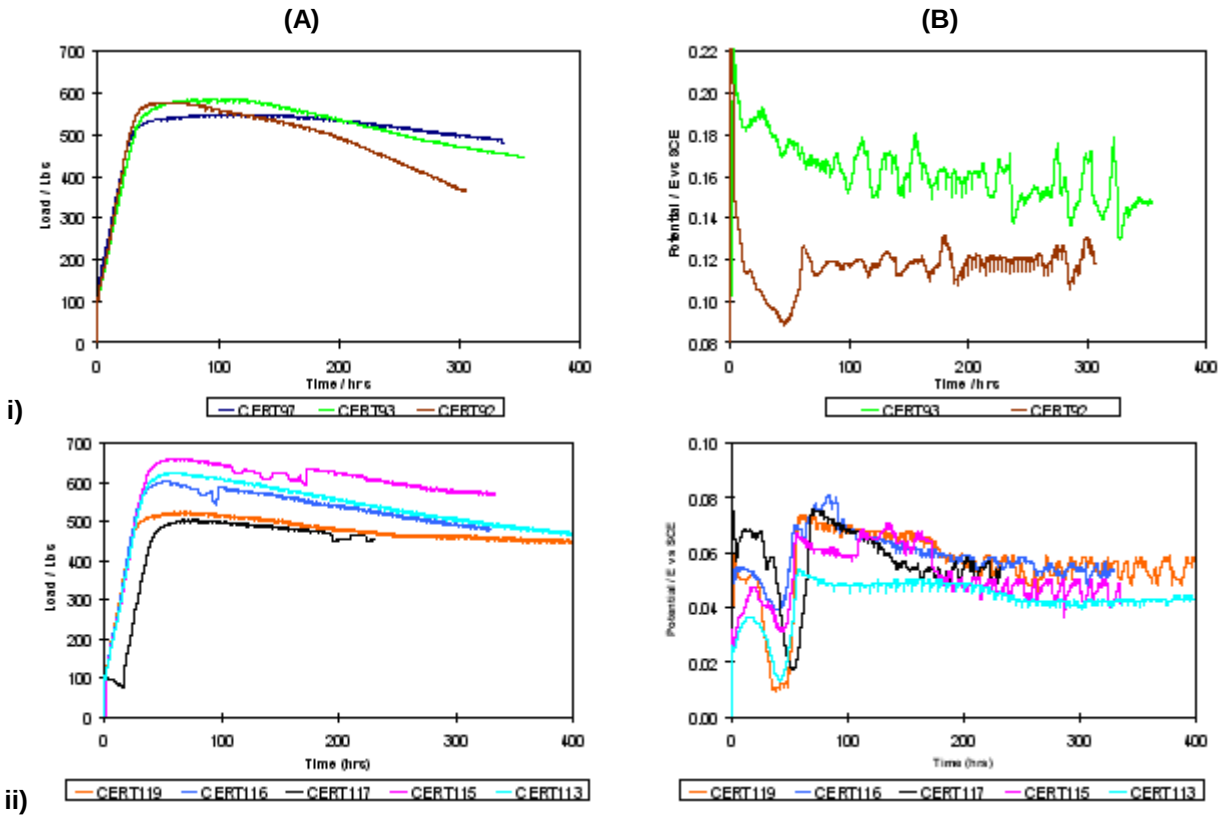

Figure 4: Graphs Showing The Effect of Acetate Concentration on Load and Potential in Deaerated Solutions Under a Galvanically Applied Current of 1 μA·cm^{-2}

Graph (A) depicts the associated load curves and graph (B) follows the associated potential-transient behaviour of i) Acetate concentrations of 0.001 mol·L^{-1} (CERT97), 0.01 mol·L^{-1} (CERT93), 0.1 mol·L^{-1} (CERT92) and ii) 0.15 mol·L^{-1} (CERT119), 0.2 mol·L^{-1} (CERT116 and CERT117), 0.3 mol·L^{-1} (CERT115) and 0.5 mol·L^{-1} (CERT113)

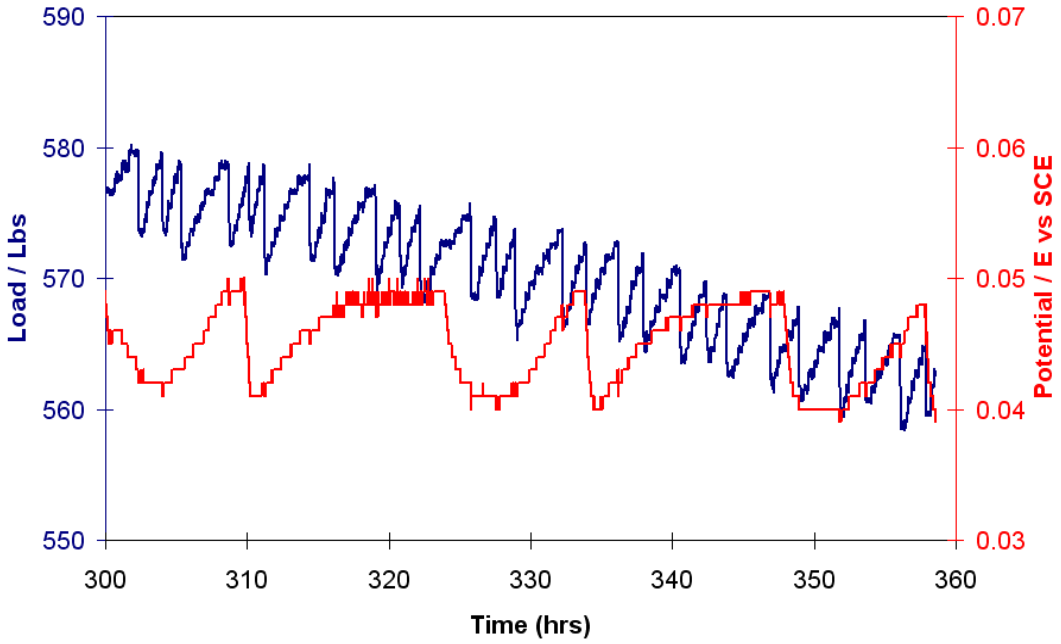

Figure 5: Graph Showing The Correlation Between The Load and Potential Transients in CERT115

Graph shows an expanded portion of the load and potential-transient curves for a deaerated 0.3 mol·L^{-1} acetate solution under a galvanically applied current of 1 μA·cm^{-2} (CERT115).

i)

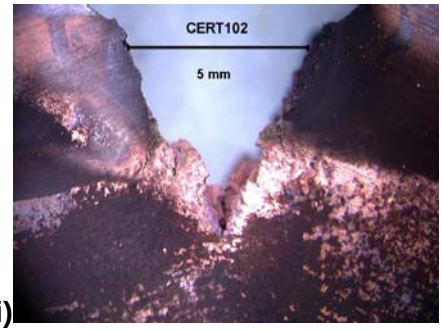

ii)

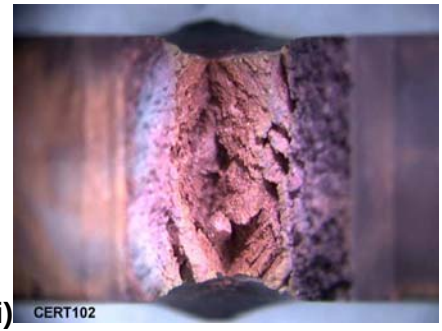

iii)

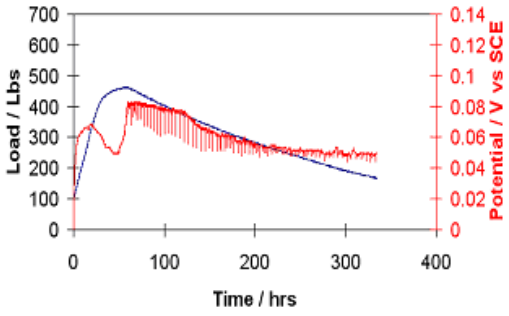

Figure 6: Macrographs and Graph of SKB4 Copper Plate Material CT Specimens Showing The Effect of the Addition of 0.001 mol·L^{-1} Chloride in 0.1 mol·L^{-1} Acetate Solution

Macrographs of CT specimen (i) surface and (ii) crack overviews (10X) following CERT in deaerated 0.1 mol·L^{-1} Acetate with 0.001 mol·L^{-1} added chloride. The scale marker represents 5 mm on the specimen. Graph (iii) depicts the associated load curves and potential-transient behaviour

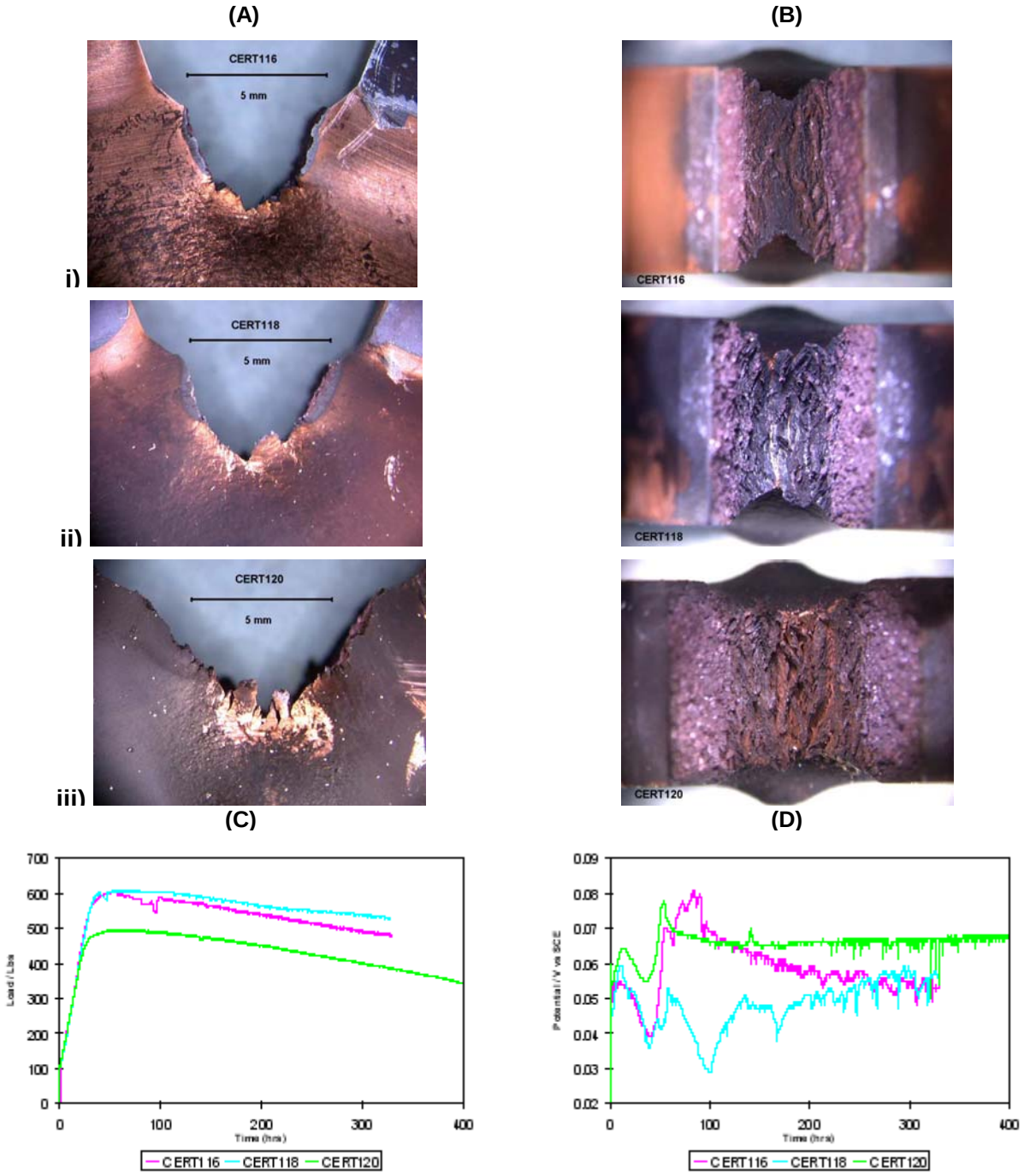

Figure 7: Macrographs and Graphs of SKB4 Copper Plate Material CT Specimens Showing The Effect of Aeration and Current Density in 0.2 mol·L^{-1} Acetate

Macrographs of CT specimen (A) surface and (B) crack overviews (10X) following CERT in 0.2 mol·L^{-1} Acetate: i) Deaerated 1 μA·cm^{-2} (CERT116), ii) Aerated 1 μA·cm^{-2} (CERT118), iii) Deaerated 2 μA·cm^{-2} (CERT120). The scale marker represents 5 mm on the specimen. Graph (A) depicts the associated load curves and graph (B) follows the associated potential-transient behaviour.

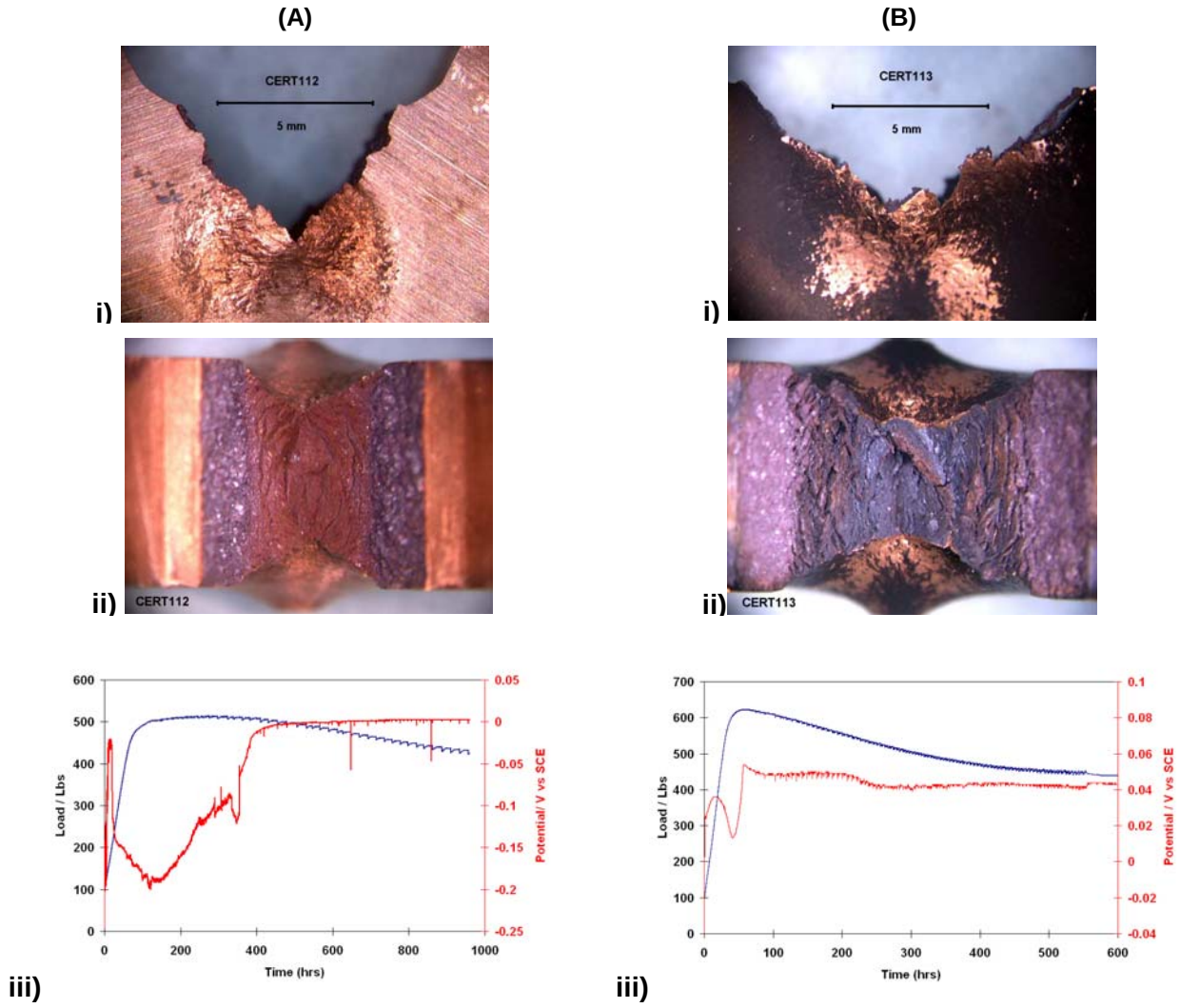

Figure 8: Macrographs and Graphs of SKB4 Copper Plate Material CT Specimens Showing The Effect of Extension Rate in 0.5 mol·L^{-1} Acetate

Macrographs of CT specimen (i) surface and (ii) crack overviews (10X) following CERT in deaerated 0.5 mol·L^{-1} Acetate at extension rates of: (A) 3.4 x 10^{-6} mm·s^{-1} (CERT112), and (B) 8.5 x 10^{-6} mm·s^{-1} (CERT113). The scale marker represents 5 mm on the specimen. Graphs (iii) depict the associated load curve and potential-transient behaviour.

Table 1: Summary of Acetate Experiments Performed* in 2008

Test Number	[Acetate] $mol \cdot L^{-1}$	pH Initial	pH Final	Atmosphere	Conditions	[Cu]† (in Solution) $mmol \cdot L^{-1}$	E_{corr} Final V	E_{red} Final V	Total Time h	K_Q $MPa \cdot m$	SCCF1	Crack Velocity $mm \cdot a^{-1}$	Crack Velocity $nm \cdot s^{-1}$
CERT112§	0.5	9.0	8.9	Deaerated	1 $\mu A/cm^2$	0.005	2	77	933.9	21.6	5.30	0.93	29.3
CERT113	0.5	9.0	8.3	Deaerated	1 $\mu A/cm^2$	0.011	43	81	622.1	24.5	4.57	2.33	73.4
CERT114#	0.3	9.0	n/a	Deaerated	1 $\mu A/cm^2$	n/a	n/a	n/a	89.2	n/a	n/a	n/a	n/a
CERT115	0.3	9.0	8.4	Deaerated	1 $\mu A/cm^2$	0.002	40	10	360.3	26.9	6.44	1.46	46.1
CERT116	0.2	9.0	8.3	Deaerated	1 $\mu A/cm^2$	0.002	51	11	334.2	25.1	4.89	2.12	66.9
CERT117	0.2	9.1	8.7	Deaerated	1 $\mu A/cm^2$	0.003	47	10	239.5	21.5	6.82	1.25	39.3
CERT118	0.2	9.0	8.7	Air	1 $\mu A/cm^2$	0.002	52	74	336.1	24.5	5.72	2.02	63.5
CERT119	0.15	9.1	8.6	Deaerated	1 $\mu A/cm^2$	0.001	55	93	503.1	23.3	5.28	2.28	71.9
CERT120	0.2	9.1	8.4	Deaerated	2 $\mu A/cm^2$	0.002	68	65	456.2	22.1	5.47	2.20	69.5

* All experiments performed in solutions at 22 ± 2°C, at a cross-head speed of 8.5×10^{-6} $mm \cdot s^{-1}$ with SKB4 compact tension specimens cut from plate, Section C1E, in a T-S orientation

§ Extension rate used was 3.4×10^{-6} $mm \cdot s^{-1}$

\# Experiment failed after 89 h

† 2σ error interval ± 10% for CERT113, CERT117 and CERT120; ± 11% for CERT115, CERT116, CERT118; and ± 13% for CERT119

Table 2: Summary of Comparative Experimental Results in All Acetate Concentrations

Test number	[Acetate] $mol \cdot L^{-1}$	Other	pH	Current $\mu A/cm^2$	SCER $(nm \cdot s^{-1})$	SCC Factor 1	SCC	Observed Crack*	Observed Surface†
CERT97	0.001	deaerated	9	1	1.80	6.54	no	ductile, blunt tip	Brown/purple oxidation, some lighter areas, less uniform
CERT93	0.01	deaerated	9	1	3.61	3.30	mix	ductile, some small SCC cracks	Bright, surface covered in blue-grey film, purple/brown oxidation in ductile zone and outward
CERT92	0.1	deaerated	9	1	2.93	4.00	mix	ductile, multiple small SCC cracks	Bright, some portions of surface covered in blue-grey film, purple oxidation around crack mouth
CERT119	0.15	deaerated	9	1	2.28	5.28	no	ductile, blunt tip, small SCC cracks	Heavy brn/blk adherent oxidation, some loosely adherent black ppte.
CERT116	0.2	deaerated	9	1	2.12	4.89	no	ductile, blunt tip, small SCC cracks	Brown tarnish, moderate brn/blk oxidation, some loosely adherent black ppte
CERT117	0.2	deaerated	9	1	1.25	6.82	no	ductile, multiple small SCC cracks	Brown tarnish, moderate brn/blk oxidation
CERT115	0.3	deaerated	9	1	1.46	6.44	no	ductile, blunt tip, small SCC cracks	Brown tarnish, heavier black oxidation with some loosely adherent black ppte.
CERT113	0.5	deaerated	9	1	2.33	4.57	no	ductile, blunt tip, small SCC cracks	Heavy, more loosely adherent black oxidation which flaked off in the ductile zone
CERT112	0.5	deaerated	9	1	0.93	5.30	no	ductile, blunt tip, small SCC cracks	Bright, surface covered in brown tarnish
CERT118	0.2	air	9	1	2.02	5.72	no	ductile, blunt tip, small SCC cracks	Heavy brn/blk adherent oxidation
CERT120	0.2	deaerated	9	2	2.20	5.47	no	ductile, multiple small SCC cracks	Heavy brn/blk adherent oxidation with some more loosely adherent ppte which flaked off in the ductile zone

* See Figures 2, 4 and 7
† See Figures 2, 3 and 7